Stability of Ferro- and Antiferromagnetism under the *s-f* Interaction*

A. J. FEDRO

Argonne National Laboratory, Argonne, Illinois and Northern Illinois University, De Kalb, Illinois

AND

TADASHI ARAI

Argonne National Laboratory, Argonne, Illinois

(Received 20 December 1967)

A system of spins interacting with each other through the *s-f* indirect exchange interaction can exhibit ferro- and antiferromagnetism alternately as a function of the Fermi momentum k_F of conduction electrons and the distance a between rare-earth atoms. This alternate behavior, however, depends critically on the *s-f* exchange parameter $\mathcal{J}_{sf}(q)$ and, if $\mathcal{J}_{sf}(q)$ decays too fast, only ferromagnetism appears. The stability condition of these states is investigated in detail, and the following conclusion is obtained: In the regions of k_Fa where the ferromagnetic energy is lower than any of the *classical* energies of antiferromagnetic states, ferromagnetism is all that can appear at all temperatures, while in other regions of k_Fa many states, including the ferromagnetic state, may be metastable, and magnetic transitions among them may be observed, but the ground state is one of antiferromagnetic states. The calculation of the stability condition resembles that of the Kohn anomalies, and hence the magnetic structures of the system is shown to be closely related to the Fermi surface.

1. INTRODUCTION

IT is generally believed that the *s-f* exchange interaction between the localized *f* electrons and conduction electrons is largely responsible for the magnetic properties of the rare-earth metals and alloys.[1] Although second-order perturbation theory of the *s-f* interaction gives the effective interaction between the *f* electrons in the form of the Heisenberg exchange Hamiltonian, this effective interaction is long range and oscillatory in real space. This long-range behavior is contrary to the short-range interaction assumed in the conventional Heisenberg theory of magnetism and makes the treatment of the *s-f* interaction more difficult. In fact, it is no longer obvious to see what type of spin arrangements appear in the ground state,[2] whereas the nature of the ground state in the simple Heisenberg model with a limited number of exchange coupling constants $\mathcal{J}$ is easily recognizable from the signs and possibly the values of the $\mathcal{J}$'s.

Mattis[3] has investigated the stability of the ferro- and antiferromagnetic states by assuming a constant *s-f* exchange parameter $\mathcal{J}_{sf}(q)$ and neglecting the anisotropic field of the crystals. This has led him to conclude that ferro- and antiferromagnetic states appear alternately as the Fermi momentum k_F of the conduction electrons is increased, or as the distances a between the rare-earth atoms are increased.

At first glance, this approximation looks reasonable, since the *f* electrons are closely bound inside the outer shells on the rare-earth atoms, and the wave functions do not overlap with each other. However, the constant $\mathcal{J}_{sf}(q)$ is quite different from more realistic interaction parameters $\mathcal{J}_{sf}(q)$ such as the one calculated by Watson and Freeman.[4] One of the objects of the present paper is to illustrate that the oscillatory behavior of having ferro- and antiferromagnetic states depends critically on the functional form of $\mathcal{J}_{sf}(q)$. The $\mathcal{J}_{sf}(q)$ obtained by Watson and Freeman decays too fast for large q and yields only the ferromagnetic state for all values of k_F and a. If the range of the $\mathcal{J}_{sf}(q)$ exceeds a certain value of q, however, the oscillatory behavior similar to that found by Mattis appears suddenly.

Mattis used the criterion that the classical energy of ferro- or antiferromagnetic states must be lower than the paramagnetic energy. He also calculated the stability requirement that the spin-wave excitation energies of the ferromagnetic state must be real and positive in the limit of long wavelengths and concluded that this requirement yields essentially the same results as the energy criterion for a large range of k_Fa values. The classical energy is obtained by replacing the spins by vectors, and it is, in fact, exact for the ferromagnetic state at $T=0$, but is an approximate one for antiferromagnetic states. From the energy comparison alone,

* Based on work performed under the auspices of the U.S. Atomic Energy Commission and a National Science Foundation Grant (GP-7330).

[1] See the review by T. Kasuya, in *Magnetism*, edited by G. Rado and H. Suhl (Academic Press Inc., New York, 1966), Vol. IIB, Chap. 3. The theory was first formulated by M. A. Ruderman and C. Kittel, Phys. Rev. **96**, 99 (1954).

[2] D. Mattis and W. Donath, Phys. Rev. **128**, 1618 (1962); D. Mattis, *ibid.* **130**, 76 (1963).

[3] D. Mattis, *The Theory of Magnetism* (Harper and Row, Publishers, Inc., New York, 1965), Chap. 7.

[4] R. E. Watson and A. J. Freeman, Phys. Rev. **152**, 566 (1966).

therefore, we cannot draw any definite conclusion as to whether the ferro- or antiferromagnetic state appears.

In the present paper, we shall rely on the expressions for the total energy $E(\mathbf{Q})$ and excitation energies $\epsilon_\nu(\mathbf{Q})$ obtained by the double-time Green function method under the Tyablikov decoupling process summarized in Sec. 3.[5] Although the antiferromagnetic energy cannot be calculated exactly, we find in Sec. 4 a very useful theorem which separates the ferromagnetic regions from regions of all other states. The theorem states that all antiferromagnetic and screw structures whose classical energies are higher than the ferromagnetic energy are unstable in the present approximation. Therefore, in the region where the ferromagnetic energy is lower than any of antiferromagnetic classical energies, ferromagnetism is all that can occur at all temperatures. According to the discussion in Sec. 5, on the other hand, several states including the ferromagnetic state can be metastable in the classically antiferromagnetic regions, and, hence, magnetic transitions among those metastable states may appear. Consequently, transitions from the ferromagnetic ground state to antiferromagnetic states are impossible in the present model in the absence of anisotropic field, but the reverse is a possibility. As is summarized in Sec. 6, energies of antiferromagnetic states will be calculated only classically, and, hence, it is not possible to draw a definite conclusion as to which one of them appears as the ground state, but the general trend of magnetic structures of the system will become quite clear.

In Secs. 4 and 5, we will also calculate the relative stability condition that excitation energies be real in the limit of long wavelengths. The formulation resembles the calculation of the Kohn anomalies in spin-wave spectra,[6,7] and the k_Fa values where an unstable state turns to a stable state can be found easily from the reciprocal lattice vectors. From the numerical results in Sec. 6, in fact, we will find that the relative stability condition yields fairly complete information as to what state becomes the ground state when a constant $\mathcal{J}_{sf}(q)$ is assumed. This suggests that there may be an intimate relation between the Fermi surface and the magnetic structure.

2. HAMILTONIAN

Let us assume that the direct interaction between f electrons is negligible, while the exchange coupling of the f electrons with the conduction electrons is given by

$$H_{sf}=-N^{-1}\sum_{n_1\mathbf{k}_1}\sum_{n_2\mathbf{k}_2}\sum_{\mathbf{l}}\mathcal{J}_{sf}(n_1\mathbf{k}_1,n_2\mathbf{k}_2)\exp[-i\mathbf{l}\cdot(\mathbf{k}_2-\mathbf{k}_1)]\times\{C_{n_2\mathbf{k}_2+}{}^{\dagger}C_{n_1\mathbf{k}_1-}S_{\mathbf{l}-}{}^{(0)}+C_{n_2\mathbf{k}_2-}{}^{\dagger}C_{n_1\mathbf{k}_1+}S_{\mathbf{l}+}{}^{(0)}+[C_{n_2\mathbf{k}_2+}{}^{\dagger}C_{n_1\mathbf{k}_1+}-C_{n_2\mathbf{k}_2-}{}^{\dagger}C_{n_1\mathbf{k}_1-}]S_{\mathbf{l}z}{}^{(0)}\}. \quad (2.1)$$

Here $C_{n\mathbf{k}\pm}$ are the Fermi destruction operators for spin $\pm\frac{1}{2}$, and $\mathcal{J}_{sf}$ is the s-f exchange integral. The $S_{\mathbf{l}}{}^{(0)}$'s are twice the ordinary Pauli spin operators (spin $\frac{1}{2}$) for the f electrons localized on lattice sites $\mathbf{l}$ ($\mathbf{l}=1\cdots N$), and satisfy the following commutation relations:

$$[S_{\mathbf{l}-}{}^{(0)},\ S_{\mathbf{l}'+}{}^{(0)}]_-=-4S_{\mathbf{l}z}{}^{(0)}\delta_{\mathbf{l}\mathbf{l}'},$$
$$[S_{\mathbf{l}\pm}{}^{(0)},\ S_{\mathbf{l}'z}{}^{(0)}]_-=\mp 2S_{\mathbf{l}\pm}\delta_{\mathbf{l}\mathbf{l}'}, \quad (2.2)$$

where

$$S_{\mathbf{l}\pm}{}^{(0)}\equiv S_{\mathbf{l}x}{}^{(0)}\pm iS_{\mathbf{l}y}{}^{(0)}. \quad (2.3)$$

The superscript (0) of the $S_{\mathbf{l}}{}^{(0)}$'s indicates that the coordinate system is fixed in the lattice.

Ordinary second-order perturbation theory yields the following effective interaction between f electrons:

$$H_{\text{eff}}=-\tfrac{1}{2}\sum_{\mathbf{l}_1}\sum_{\mathbf{l}_2(\neq\mathbf{l}_1)}J(\mathbf{l}_1-\mathbf{l}_2)\mathbf{S}_{\mathbf{l}_1}{}^{(0)}\cdot\mathbf{S}_{\mathbf{l}_2}{}^{(0)}, \quad (2.4)$$

with

$$J(\mathbf{l}_1-\mathbf{l}_2)=\left(\frac{1}{N}\right)^2\sum_{n_1\mathbf{k}_1}\sum_{n_2\mathbf{k}_2}\frac{\mathcal{J}_{sf}{}^2(n_1\mathbf{k}_1;\,n_2\mathbf{k}_2)f_{n_1\mathbf{k}_1}}{\epsilon_{n_2\mathbf{k}_2}-\epsilon_{n_1\mathbf{k}_1}}\times\exp[i(\mathbf{k}_2-\mathbf{k}_1)\cdot(\mathbf{l}_1-\mathbf{l}_2)]. \quad (2.5)$$

Here

$$f_{n\mathbf{k}}=\{1+\exp[\beta(\epsilon_{n\mathbf{k}}-\mu)]\}^{-1} \quad (2.6)$$

with $\beta=1/k_BT$, μ the Fermi energy, and $\epsilon_{n\mathbf{k}}$ is the one-electron energy of the conduction electron with momentum $\mathbf{k}$ and band index n in the reduced zone scheme.

In this paper we shall limit our discussion to the system of spins interacting with each other by the effective spin Hamiltonian H_{eff} and neglect the direct effect of the s-like conduction bands to the magnetic properties. For convenience, we shall further assume that the f electrons occupy sites on a simple cubic lattice of spacing a. Systems of this type, for example, are found in the rare earth-noble metal intermetallic compounds having the CsCl structure.

It is convenient to describe the various spin configurations observed in the lattice by using rotating coordinate systems. The components $S_{\mathbf{l}x}{}^{(0)}$, $S_{\mathbf{l}y}{}^{(0)}$, and $S_{\mathbf{l}z}{}^{(0)}$ in the fixed coordinate system (x, y, z) is then transformed to the rotating system (x', y', z') with pitch $\mathbf{Q}$ as follows:

$$S_{\mathbf{l}x}{}^{(0)}=-\sin(\mathbf{Q}\cdot\mathbf{l})\ S_{\mathbf{l}y'}{}^{(\mathbf{Q})}+\cos(\mathbf{Q}\cdot\mathbf{l})\ S_{\mathbf{l}z'}{}^{(\mathbf{Q})},$$
$$S_{\mathbf{l}y}{}^{(0)}=\cos(\mathbf{Q}\cdot\mathbf{l})\ S_{\mathbf{l}y'}{}^{(\mathbf{Q})}+\sin(\mathbf{Q}\cdot\mathbf{l})\ S_{\mathbf{l}z'}{}^{(\mathbf{Q})},$$
$$S_{\mathbf{l}z}{}^{(0)}=-S_{\mathbf{l}x'}{}^{(\mathbf{Q})}, \quad (2.7)$$

where the $S^{(\mathbf{Q})}$'s also satisfy the commutation relations (2.2), and $\mathbf{Q}\cdot\mathbf{l}$ is the angle in the fixed x-y plane that the z' axis makes with the fixed x axis. Substitution of

[5] See, for instance, S. V. Tyablikov, *Method in the Quantum Theory of Magnetism* (Plenum Press, New York, 1967), Chap. VIII.

[6] W. Kohn, Phys. Rev. Letters **2**, 393 (1959).

[7] E. J. Woll, Jr., and S. J. Nettel, Phys. Rev. **123**, 796 (1961).

Eq. (2.7) into Eq. (2.4) yields the Hamiltonian in the rotating coordinate systems.

$$H_{\text{eff}}=-\tfrac{1}{2}\sum_{l_1,l_2}{}'J(l_1-l_2)\{-\tfrac{1}{2}[\sin^2\tfrac{1}{2}\mathbf{Q}\cdot(l_1-l_2)]\times[S_{l_1+}{}^{(\mathbf{Q})}S_{l_2+}{}^{(\mathbf{Q})}+S_{l_1-}{}^{(\mathbf{Q})}S_{l_2-}{}^{(\mathbf{Q})}]+\tfrac{1}{2}[\cos^2\tfrac{1}{2}\mathbf{Q}\cdot(l_1-l_2)][S_{l_1+}{}^{(\mathbf{Q})}S_{l_2-}{}^{(\mathbf{Q})}+S_{l_1-}{}^{(\mathbf{Q})}S_{l_2+}{}^{(\mathbf{Q})}]+(1/2i)[\sin\mathbf{Q}\cdot(l_1-l_2)]\times[(S_{l_1+}{}^{(\mathbf{Q})}-S_{l_1-}{}^{(\mathbf{Q})})S_{l_2z}{}^{(\mathbf{Q})}-S_{l_1z}{}^{(\mathbf{Q})}(S_{l_2+}{}^{(\mathbf{Q})}-S_{l_2-}{}^{(\mathbf{Q})})]+[\cos\mathbf{Q}\cdot(l_1-l_2)]S_{l_1z}{}^{(\mathbf{Q})}S_{l_2z}{}^{(\mathbf{Q})}\}. \quad (2.8)$$

3. SOLUTION OF THE GREEN'S FUNCTIONS

We turn in this section to the definition and method of solution of the relevant Green's functions. As in Bonch-Bruevich and Tyablikov[8] we define the Green's functions involving the Heisenberg operators $A(t)$ and $B(t)$ as follows:

$$\langle\langle A(t)\mid B(t')\rangle\rangle\equiv i\theta(t-t')\langle[A(t),B(t')]_-\rangle, \quad (3.1)$$

where $\langle\cdots\rangle$ represents an average over a canonical ensemble, $\theta(t)$ a step function, and $[\ ]_-$ a commutator. The equation of motion is then

$$E\langle\langle A\mid B\rangle\rangle_E=-(1/2\pi)\langle[A,B]_-\rangle-\langle\langle[H,A]_-\mid B\rangle\rangle_E, \quad (3.2)$$

where $\langle\langle\mid\rangle\rangle_E$ is the energy Fourier transform of $\langle\langle\mid\rangle\rangle$. The correlation function can then be written as

$$\langle A(t)B(t')\rangle=\int_{-\infty}^{\infty}dE\exp[-iE(t-t')]\times\{1-\exp(-\beta E)\}^{-1}\times\{\lim_{\epsilon\to 0}(-i)[\langle\langle A\mid B\rangle\rangle_{E+i\epsilon}-\langle\langle A\mid B\rangle\rangle_{E-i\epsilon}]\}. \quad (3.3)$$

We need to compute Green's functions of the type

$$\langle\langle S_{l_1a}{}^{(\mathbf{Q})}(t)\mid S_{l_2b}{}^{(\mathbf{Q})}(t')\rangle\rangle, \qquad a,b=z,+,-. \quad (3.4)$$

Setting up the equation of motion for the above functions using Eqs. (2.8) and (3.2), we find a closed set of equations under the following chain-breaking approximations:

$$\langle\langle A(t)B(t)\mid C(t')\rangle\rangle\approx\langle A\rangle\langle\langle B(t)\mid C(t')\rangle\rangle+\langle B\rangle\langle\langle A(t)\mid C(t')\rangle\rangle, \quad (3.5)$$

where we will demand in state $\mathbf{Q}$ that $\langle S_{l_z}{}^{(\mathbf{Q})}\rangle=\sigma(\mathbf{Q})$ and $\langle S_{l\pm}{}^{(\mathbf{Q})}\rangle=0$. The result is reduced to a 2×2 set of equations among the $\langle\langle S_{l\sigma}{}^{(\mathbf{Q})}(t)\mid S_{l'\sigma'}{}^{(\mathbf{Q})}(t')\rangle\rangle$ with $\sigma=+,-$, since the functions $\langle\langle S_{lz}{}^{(\mathbf{Q})}(t)\mid S_{l'\pm}{}^{(\mathbf{Q})}(t')\rangle\rangle$ vanish under these approximations. We solve in the normal way by searching for solutions of the type

$$\langle\langle S_{l\sigma}{}^{(\mathbf{Q})}\mid S_{l'\sigma'}{}^{(\mathbf{Q})}\rangle\rangle_E=N^{-1}\sum_{\nu}\exp[i\nu\cdot(l-l')]G_\nu{}^{\sigma\sigma'}(\mathbf{Q};E), \quad (3.6)$$

where the ν's are wave vectors contained in the first Brillouin zone of the lattice reciprocal to the space lattice. The solutions are

$$G_\nu{}^{+-}(\mathbf{Q};E)=G_\nu{}^{-+}(\mathbf{Q};-E)=[-2\sigma(\mathbf{Q})/\pi]\{[E+F_\nu(\mathbf{Q})]/[E^2-\epsilon_\nu{}^2(\mathbf{Q})]\}; \quad (3.7)$$

$$G_\nu{}^{++}(\mathbf{Q};E)=G_\nu{}^{--}(\mathbf{Q};E)=[-2\sigma(\mathbf{Q})/\pi]\{B_\nu(\mathbf{Q})/[E^2-\epsilon_\nu{}^2(\mathbf{Q})]\}. \quad (3.8)$$

We have made the following definitions:

$$F_\nu(\mathbf{Q})=2\sigma(\mathbf{Q})[I(\mathbf{Q})-\tfrac{1}{2}I(\nu)-\tfrac{1}{4}(\mathbf{Q}+\nu)-\tfrac{1}{4}I(\mathbf{Q}-\nu)], \quad (3.9a)$$

$$B_\nu(\mathbf{Q})=2\sigma(\mathbf{Q})[\tfrac{1}{2}I(\nu)-\tfrac{1}{4}I(\mathbf{Q}+\nu)-\tfrac{1}{4}I(\mathbf{Q}-\nu)], \quad (3.9b)$$

$$\epsilon_\nu(\mathbf{Q})=\{F_\nu{}^2(\mathbf{Q})-B_\nu{}^2(\mathbf{Q})\}^{1/2}=2\sigma(\mathbf{Q})\{[I(\mathbf{Q})-I(\nu)]\times[I(\mathbf{Q})-\tfrac{1}{2}I(\mathbf{Q}+\nu)-\tfrac{1}{2}I(\mathbf{Q}-\nu)]\}^{1/2}, \quad (3.9c)$$

with

$$I(\mathbf{P})=\sum_{l\neq0}J(l)e^{i\mathbf{P}\cdot l}, \quad (3.10)$$

and $\sigma(\mathbf{Q})$ determined self-consistently by the relation

$$[\sigma(\mathbf{Q})]^{-1}=N^{-1}\sum_{\nu}[F_\nu(\mathbf{Q})/\epsilon_\nu(\mathbf{Q})]\coth\tfrac{1}{2}\beta\epsilon_\nu(\mathbf{Q}). \quad (3.11)$$

The average energy $E(\mathbf{Q})$ is then

$$E(\mathbf{Q})=E'(\mathbf{Q})+E''(\mathbf{Q}), \quad (3.12)$$

with the classical energy $E'(\mathbf{Q})$ given by

$$E'(\mathbf{Q})=-\tfrac{1}{2}NI(\mathbf{Q}), \quad (3.13a)$$

and the quantum effect $E''(\mathbf{Q})$ given by

$$E''(\mathbf{Q})=-\tfrac{1}{2}N[\sigma^2(\mathbf{Q})-1]I(\mathbf{Q})-\tfrac{1}{2}\sigma(\mathbf{Q})\sum_{\nu}[I(\nu)+\tfrac{1}{2}I(\mathbf{Q}+\nu)+\tfrac{1}{2}I(\mathbf{Q}-\nu)]\times[F_\nu(\mathbf{Q})/\epsilon_\nu(\mathbf{Q})]\coth\tfrac{1}{2}\beta\,\epsilon_\nu(\mathbf{Q})-\tfrac{1}{2}\sum_{\nu}[B_\nu{}^2(\mathbf{Q})/\epsilon_\nu(\mathbf{Q})]\coth\tfrac{1}{2}\beta\,\epsilon_\nu(\mathbf{Q}). \quad (3.13b)$$

At this point it is convenient to separate the discussion of the various ordered states into two parts, that for the ferromagnetic state $\mathbf{Q}=0$ and those for the antiferromagnetic and screw structure states $\mathbf{Q}\neq0$.

[8] V. L. Bonch-Bruevich and S. V. Tyablikov, *The Green Function Method in Statistical Mechanics* (North-Holland Publishing Co., Amsterdam, 1962).

4. FERROMAGNETIC STATE (Q=0)

Here we shall investigate the stability of the ferromagnetic state. In general, for a state Q to be the ground state, it is necessary to show either that (a) the excitation energies $\epsilon_\nu(\mathbf{Q})$ are positive definite for all ν, or that (b) the total energy $E(\mathbf{Q})$ is the lowest among all possible spin states. We must also show that the magnetization $\sigma(\mathbf{Q})$ is nonvanishing and positive, so that the ground state has, in fact, the desired long-range spin arrangement. For the ferromagnetic ground state, the stability condition (a) is given by

$$I(0)-I(\nu)\geq 0, \tag{4.1}$$

for all ν, as is obtained from Eq. (3.9).

It is not feasible, however, to calculate the validity of the above inequality for all ν, and, hence, we shall limit in this paper the discussion of Eq. (4.1) to *small* ν and call it the *relative* stability condition. To supplement this limitation, we also calculate a part of the second condition (b), that is, (b_1) the total energy $E(\mathbf{Q})$ is lower than the paramagnetic energy at $T=0$, and (b_2) the energy is in fact minimum among the finite number of states considered in this paper. For the ferromagnetic state, the requirement (b_1) is written as

$$I(0)>0, \tag{4.2}$$

using Eqs. (3.12) and (3.13) together with the fact that the paramagnetic energy is taken to be zero in the present description. The classical energy comparison between the ferro and the three types of antiferromagnetic states considered will be carried out numerically and will be discussed in the following two sections.

One might feel uncertain in doing such comparison of energies of distinct states. In fact, the values of the antiferromagnetic energies evaluated classically are higher than the exact energies, while the ferromagnetic energy is calculated exactly at $T=0$, and, hence, the classical energy comparison is always unfavorable for the antiferromagnetic states. Fortunately, the following theorem will eliminate this difficulty.

Theorem: If the ferromagnetic state satisfies the relative stability condition (4.1) for *small* ν, and if the exact ferromagnetic energy is lower than the classical energies $E'(\mathbf{Q})$ of an antiferromagnetic state or screw structure state Q, then the state Q becomes unstable against small deformations under the present approximation.

Consequences of this theorem are that, if the ferromagnetic state is the ground state, no other states can be metastable, and thus, it is not possible to expect any magnetic transition from the ferromagnetic state to antiferromagnetic or screw structure states under the *s-f* interaction in the absence of anisotropic fields. Whether or not the ferromagnetic state is the ground state can also be decided by comparing its energy with the classical energies $E'(\mathbf{Q})$ of all other possible states. As we shall discuss in Sec. 6, the reverse of the theorem is not true, and, so if an antiferromagnetic state is the ground state, the ferromagnetic or other states may be metastable, and, hence, magnetic transitions to such metastable states may be possible.

The theorem can be proved as follows. For a state Q to be metastable, the energy must be a minimum, at least, in the vicinity of Q. In classical approximation, this yields

$$I(\mathbf{Q})-\tfrac{1}{2}I(\mathbf{Q}+\nu)-\tfrac{1}{2}I(\mathbf{Q}-\nu)>0, \qquad \text{for small } \nu, \tag{4.3}$$

while, by assumption, the classical energy $E'(\mathbf{Q})$ of the state Q is higher than the ferromagnetic energy $E(0)$, and, hence,

$$I(\mathbf{Q})-I(0)<0. \tag{4.4a}$$

For small ν, the inequality is essentially equivalent to

$$I(\mathbf{Q})-I(\nu)<0, \tag{4.4b}$$

because the difference $I(\nu)-I(0)$ vanishes in the limit of small ν. Use of Eqs. (4.3) and (4.4b) in Eq. (3.9c) leads to the conclusion that excitation energies of the state Q are imaginary in the limit of small ν, illustrating the instability of the state Q against small deformations.

To calculate the stability conditions (4.1) and (4.2) of the ferromagnetic state explicitly, we shall develop an expansion method for the calculation of $I(\nu)$. Use of Eq. (2.5) into Eq. (3.10) yields the explicit expression of $I(\nu)$, but to compute it, we need to assume the behavior of $I(\nu)$ to be well approximated by the following two simplifications: (1) Wave functions for electrons in the conduction bands can be given by plane waves. Hence,

$$I(\nu)=\left(\frac{1}{N}\right)^2\sum_{\mathbf{l}\neq 0}\sum_{\mathbf{k}',\mathbf{k}}\frac{\mathcal{J}_{sf}^2(\mathbf{k},\mathbf{k}')f_{\mathbf{k}}}{(\hbar^2/2m^*)(k'^2-k^2)}\times\exp[i(\mathbf{k}'-\mathbf{k}-\nu)\cdot\mathbf{l}], \tag{4.5}$$

where the band indices are removed and instead the unlimited $\mathbf{k}$'s are used. (2) The $\mathcal{J}_{sf}(\mathbf{k},\mathbf{k}')$ depends only on $|\mathbf{k}'-\mathbf{k}|$ and can thus be written

$$\mathcal{J}_{sf}(\mathbf{k},\mathbf{k}')=\mathcal{J}_{sf}(|\mathbf{k}'-\mathbf{k}|). \tag{4.6}$$

This is Kasuya's assumption,[9] but Overhauser[10] has proved that this approximation becomes rigorous when a δ-function potential replaces the Coulomb potential in $\mathcal{J}_{sf}$. More recently, Watson and Freeman[4] have shown that the rigorous calculation of $\mathcal{J}_{sf}$ by the use of orthogonalized-plane-wave (OPW) and Hartree–Fock atomic functions yield the approximate relation (4.6) quite well, at least for Gd.

Let κ be the reciprocal lattice vectors appropriate to the space lattice. Then the index $\mathbf{k}'$ in Eq. (4.5) must

[9] T. Kasuya, Progr. Theoret. Phys. (Kyoto) **16**, 45 (1956).
[10] A. W. Overhauser, J. Appl. Phys. **34**, 1019 S (1963).

satisfy the relation

$$\mathbf{k}'=\mathbf{k}+\boldsymbol{\nu}+\boldsymbol{\kappa}. \tag{4.7}$$

Use of Eqs. (4.6) and (4.7) in Eq. (4.5) yields

$$I(\boldsymbol{\nu})=(k_Fa)D\{\sum_{\kappa}\mathcal{J}_{sf}^2(|\boldsymbol{\nu}+\boldsymbol{\kappa}|)U(|\boldsymbol{\nu}+\boldsymbol{\kappa}|;T)\}-J(0), \tag{4.8}$$

where

$$U(|\boldsymbol{\nu}+\boldsymbol{\kappa}|;T)=[k_F(|\boldsymbol{\nu}+\boldsymbol{\kappa}|)]^{-1}\times\int_0^{\infty}dk\,kf_K\ln\left|\frac{2k+|\boldsymbol{\nu}+\boldsymbol{\kappa}|}{2k-|\boldsymbol{\nu}+\boldsymbol{\kappa}|}\right|, \tag{4.9}$$

where

$$D=\frac{m^*V}{8\pi^2\hbar^2aN} \tag{4.10}$$

and where k_F is the Fermi momentum. The self-energy term $J(0)\neq 0$ is subtracted in Eq. (4.8) because it is excluded in the definition (3.10) of $I(\boldsymbol{\nu})$ while the first term on the right of (4.8) automatically includes it. When $T=0$, the Fermi function k_F can be replaced by a step function, and the integration involved in $U(|\boldsymbol{\nu}+\boldsymbol{\kappa}|;T=0)$ can be carried out explicitly yielding

$$U(|\boldsymbol{\nu}+\boldsymbol{\kappa}|;T=0)\equiv U(|\boldsymbol{\nu}+\boldsymbol{\kappa}|/2k_F)=\frac{1}{2}\left\{1+\frac{(1-x^2)}{2x}\ln\left|\frac{x+1}{x-1}\right|\right\}, \tag{4.11}$$

where

$$x=|\boldsymbol{\nu}+\boldsymbol{\kappa}|/2k_F. \tag{4.12}$$

Since the temperature dependence of $U(|\boldsymbol{\nu}+\boldsymbol{\kappa}|;T)$ is shown to be very weak, $U(|\boldsymbol{\nu}+\boldsymbol{\kappa}|;T)$ can be well approximated by $U(|\boldsymbol{\nu}+\boldsymbol{\kappa}|/2k_F)$. Consequently $I(\boldsymbol{\nu})$ can be regarded as a temperature-independent quantity given by

$$I(\boldsymbol{\nu})=(k_Fa)D\{\sum_{\kappa}\mathcal{J}_{sf}^2(|\boldsymbol{\nu}+\boldsymbol{\kappa}|)U(|\boldsymbol{\nu}+\boldsymbol{\kappa}|/2k_F)-N^{-1}\sum_{\kappa}\mathcal{J}_{sf}^2(k)U(k/2k_F)\}. \tag{4.13}$$

Thus our relative stability and energy conditions read

$$I(0)-I(\boldsymbol{\nu})=(k_Fa)D\{\sum_{\kappa}[\mathcal{J}_{sf}^2(\kappa)U(\kappa/2k_F)-\mathcal{J}_{sf}^2(|\boldsymbol{\nu}+\boldsymbol{\kappa}|)U(|\boldsymbol{\nu}+\boldsymbol{\kappa}|/2k_F)]\}\geq 0, \tag{4.14}$$

and

$$I(0)=(k_Fa)D\{\sum_{\kappa}\mathcal{J}_{sf}^2(\kappa)U(\kappa/2k_F)-N^{-1}\sum_{\kappa}\mathcal{J}_{sf}^2(k)U(k/2k_F)\}>0. \tag{4.15}$$

We can now show that the assumed functional form of $\mathcal{J}_{sf}(q)$ is critical for satisfying the relative stability and energy conditions (4.14) and (4.15) for the ferromagnetic state. We shall examine three cases.

Case 1. Kasuya's $\mathcal{J}_{sf}(q)$

In line with Kasuya[9] we shall assume that $\mathcal{J}_{sf}(q)$ behaves as follows: When q is much smaller then the first reciprocal lattice vector $\boldsymbol{\kappa}_1$, $\mathcal{J}_{sf}(q)$ decreases slowly as q increases, but as q approaches a critical value which is close to but smaller than κ_1, $\mathcal{J}_{sf}(q)$ starts to decrease rapidly and becomes negligible for $q>|\kappa_1|$. Then the conditions (4.14) and (4.15) become

$$I(0)-I(\boldsymbol{\nu})=(k_Fa)D\times\{\mathcal{J}_{sf}^2(0)U(0)-\mathcal{J}_{sf}^2(\nu)U(\nu/2k_F)\}\geq 0, \tag{4.16}$$

and

$$I(0)=(k_Fa)D\times\{\mathcal{J}_{sf}^2(0)U(0)-N^{-1}\sum_{\kappa}^{|\mathbf{k}|\leq|\boldsymbol{\kappa}_1|}\mathcal{J}_{sf}^2(k)U(k/2k_F)\}>0, \tag{4.17}$$

so that the ferromagnetic state is stable for all values of k_Fa.

Case 2. $\mathcal{J}_{sf}(q)=\mathcal{J}_{sf}(0)=$ const. for all q

In contrast to case 1, we find that the conditions (4.14) and (4.15) are not always satisfied, so that ferromagnetism is not always possible. According to the numerical analysis of the semiclassical approach by Mattis,[3] one finds alternating regions where the stability conditions are satisfied and violated. This suggests that some type of antiferromagnetic ordering is taking place in the appropriate regions.

Here we shall investigate the stability condition (4.14) analytically in the limit of small $\boldsymbol{\nu}$. For small $\boldsymbol{\nu}$ a Taylor series expansion of Eq. (4.14) yields

$$I(0)-I(\boldsymbol{\nu})\cong\tfrac{1}{3}[(k_Fa)D]\mathcal{J}_{sf}^2(0)\times\{1-\sum_{\kappa\neq 0}\tfrac{1}{2}[g(\kappa)]G(\kappa/2k_F)\}(\nu/2k_F)^2\geq 0, \tag{4.18}$$

where

$$G(x)=[2U'(x)/x]+U''(x);\qquad x\equiv\kappa/2k_F, \tag{4.19}$$

and $g(\kappa)$ is the number of reciprocal lattice vectors with a constant magnitude $|\boldsymbol{\kappa}|$ while the prime superscripts over $U(x)$ denote differentiation with respect to the argument. The relative stability condition (4.18) is then written

$$1-\tfrac{1}{2}\sum_{\kappa\neq 0}g(\kappa)G(\kappa/2k_F)>0. \tag{4.20}$$

We must be careful in applying the condition (4.20). As is shown in Fig. 1, $G(x)$ diverges at $x=1$, and the Taylor expansion breaks down in the vicinity of the singularity, but we still find that the expansion (4.18) is an excellent approximation to (4.14) for small $\boldsymbol{\nu}$ when $|1-x|\gtrsim 0.05$. We note that the divergence of $G(\kappa/2k_F)$ yields kinks in the spin-wave dispersion curve which are known as the Kohn anomalies.[6] In the limit

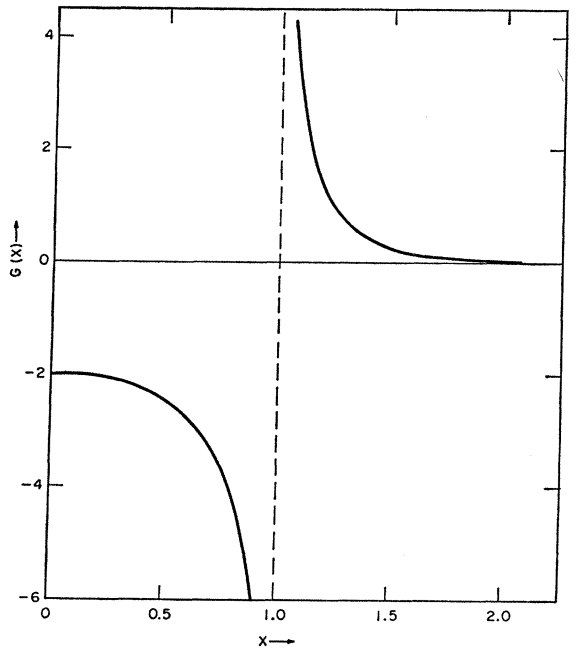

FIG. 1. Plot of $G(x)=(2/x)\partial U/\partial x+\partial^2 U/\partial x^2$, where $x\equiv\kappa/2k_F$ and $U(x)\equiv\frac{1}{2}\{1+[(1-x^2)/2x]\ln|(x+1)/(x-1)|\}$.

of long wavelengths $\nu\to 0$, such kinks may shift a spin-wave dispersion curve upwards (downwards) and change the otherwise negative (positive) sign of the curve to positive (negative). If this situation occurs, the Kohn anomaly is considered to be responsible for the stability of ferromagnetism, and, in turn, the resulting stability becomes intimately related to the Fermi surface through the value of the Fermi momentum k_F.

Let us illustrate this situation more explicitly by evaluating the expression on the left of Eq. (4.20). In our simple cubic lattice the values κ are given by

$$\kappa=(2\pi/a)(n_1^2+n_2^2+n_3^2)^{1/2}, \qquad (4.21)$$

where n_1, n_2, and n_3 are integers, and $n_1=n_2=n_3=0$ is not included. Since the minimum values of κ is $2\pi/a$, the values of $G(\kappa/2k_F)$ for all κ are found to be positive as long as $k_Fa<\pi$. In particular, for small k_Fa, all the $G(\kappa/2k_F)$ are small and the sum $\frac{1}{2}\sum_\kappa g(\kappa)G(\kappa/2k_F)$ converges to a value less than one. The condition (4.20) is then satisfied, and a positive dispersion curve results. However, as the value of k_Fa approaches 2.0, the sum becomes greater than 1, and the inequality relation (4.20) breaks down. The resulting instability persists in the region $2.0\leq k_Fa\leq\pi$. As the value of k_Fa becomes greater than π, the first term in the sum $\frac{1}{2}g(\kappa_1)G(\kappa_1/2k_F)$ which involves the first nonzero set of reciprocal lattice vectors $\boldsymbol{\kappa}_1$ and is the dominant term in the sum, changes sign while the rest of the $G(\kappa/2k_F)$'s stays small. This results in the change of sign of the slope of the dispersion curve to plus, and represents the kink passing through the origin. Again then the condition (4.20) is satisfied yielding stability of ferromagnetism. With a further increase of k_Fa, this condition is again violated at around $k_Fa\approx 3.8$, since the negative contribution from the second set κ_2 of reciprocal lattice vectors becomes dominant. As $k_Fa\gtrsim\sqrt{2}\pi$, the sign of this second term changes and passing through the resulting Kohn anomaly stabilizes ferromagnetism, etc. This oscillatory behavior persists with the bringing-in of higher sets of reciprocal lattice vectors $\boldsymbol{\kappa}$ inside of the singularity. In fact, we have calculated the expression to the left of Eq. (4.20) numerically, and the result is summarized in Sec. 6.

We also calculate $I(0)$ numerically and plot the values versus k_Fa. From these results we will find that the regions where the energy condition (4.15) is satisfied is essentially the same as the region obtained from the relative stability condition (4.20).

Case 3. General $\mathcal{J}_{sf}(q)$

Watson and Freeman[4] have used more realistic methods for determining $\mathcal{J}_{sf}(q)$ and concluded that the actual situation lies between the limiting cases 1 and 2. The realistic $\mathcal{J}_{sf}(q)$ is considered as a decaying and oscillating function of q. The expression (4.14) for small ν can then be expanded as:

$$\begin{aligned}I(0)-I(\nu)\cong(k_Fa)D[&\{\tfrac{1}{3}\mathcal{J}_{sf}^2(0)-\sum_{\kappa\neq 0}\tfrac{1}{6}\mathcal{J}_{sf}^2(\kappa)g(\kappa)G(\kappa/2k_F)\}(\nu/2k_F)^2\\&+\{-2\mathcal{J}_{sf}(0)\,(2k_F\mathcal{J}_{sf}'(0)\,)(\nu/2k_F)-\tfrac{2}{3}\sum_{\kappa\neq 0}\mathcal{J}_{sf}(\kappa)\,(2k_F\mathcal{J}_{sf}'(\kappa)\,)g(\kappa)H(\kappa/2k_F)(\nu/2k_F)^2\}\\&+\{-[\mathcal{J}_{sf}(0)\,((2k_F)^2\mathcal{J}_{sf}''(0)\,)+(2k_F\mathcal{J}_{sf}'(0)\,)^2]\\&-\tfrac{1}{3}\sum_{\kappa\neq 0}[\mathcal{J}_{sf}(\kappa)\,((2k_F)^2\mathcal{J}_{sf}''(\kappa)\,)+(2k_F\mathcal{J}_{sf}'(\kappa)\,)^2]g(\kappa)U(\kappa/2k_F)\}(\nu/2k_F)^2]\geq 0, \qquad (4.22)\end{aligned}$$

where the function

$$H(x)=[U(x)/x]+U'(x) \qquad (4.23)$$

also has a singularity at $x=1$ as is illustrated in Fig. 2. If the derivative of $\mathcal{J}_{sf}(q)$ at $q=0$, $\mathcal{J}_{sf}'(0)$ is negative, then the first part of the second term on the right of Eq. (4.22) becomes dominant, since this part is proportional to ν. The condition (4.22) is then satisfied, and we only need to investigate the energy condition (4.15). If, on the other hand, $\mathcal{J}_{sf}'(0)$ is positive, ferromagnetism is obviously unstable. However, $\mathcal{J}_{sf}'(0)$ is normally taken as zero, and the major contributions to the in-

equality (4.22) appear from the constant term $\frac{1}{3}[\mathcal{J}_{sf}^2(0)]$ and terms involving $G(x_n)$ and $H(x_n)$ where the values of x_n are in the vicinity of the singularities of these functions. The relative stability condition (4.22) is then simplified to

$$1-\tfrac{1}{2}\sum_{\kappa_n}[\mathcal{J}_{sf}(\kappa_n)/\mathcal{J}_{sf}(0)]^2 g(\kappa_n)\mathcal{G}(\kappa_n/2k_F)>0, \quad (4.24)$$

where

$$\mathcal{G}(\kappa_n/2k_F)=G(\kappa_n/2k_F) +4[2k_F\mathcal{J}_{sf}'(\kappa_n)/\mathcal{J}_{sf}(\kappa_n)]H(\kappa_n/2k_F). \quad (4.25)$$

We note that the third term in Eq. (4.22) does not have a singularity and hence does not contribute significantly to (4.24).

As long as $\mathcal{J}_{sf}(\kappa)$ varies gradually and the value of $[2k_F\mathcal{J}_{sf}'(\kappa)/\mathcal{J}_{sf}(\kappa)]$ is not exceedingly large, the first term in (4.25), $G(\kappa/2k_F)$ will dominate over the second term, and $\mathcal{G}(\kappa/2k_F)$ will resemble $G(\kappa/2k_F)$. The condition (4.24) is then similar to (4.20) and will, in principle, exhibit alternating regions of k_Fa where the inequality (4.24) is satisfied and violated. If the $\mathcal{J}_{sf}(\kappa_n)$ decays with increasing κ_n so that

$$|\mathcal{J}_{sf}(\kappa_n)/\mathcal{J}_{sf}(0)|<1,$$

the contribution from the sum on the left of Eq. (4.24) will decrease as compared with the corresponding term in Eq. (4.20). In fact, the value of the sum will remain less than 1 at $k_Fa\approx 2.0$, so that the first region of ferromagnetism becomes somewhat wider but cuts out before $k_Fa=\pi$. At $k_Fa\gtrsim\pi$, the first term of the sum, $g(\kappa_1)\mathcal{G}(\kappa_1/2k_F)$, changes sign, and the accompanying Kohn anomaly puts the system back to ferromagnetism just as in Eq. (4.20). Since $|\mathcal{J}_{sf}(\kappa_2)/\mathcal{J}_{sf}(0)|$ is still smaller than $|\mathcal{J}_{sf}(\kappa_1)/\mathcal{J}_{sf}(0)|$, this second ferromagnetic region may become even wider until we find that the relative stability condition for the ith region will continue up to the $(i+1)$th region except in the narrow vicinity of the singularity of $G(\kappa_i/2k_F)$. In this region the Taylor expansion used in obtaining Eq. (4.22) is invalid, and the instability is merely a fictitious one. Beyond the ith region, therefore, ferromagnetism must be stable for all k_Fa. This tendency will be accelerated if $\mathcal{J}_{sf}(q)$ decreases faster, until we find in the Kasuya limit, where $i=1$ that ferromagnetism is stable for all k_Fa.

5. ANTIFERROMAGNETIC STATES ($\mathbf{Q}\neq 0$)

Since many antiferromagnetic or screw structures which have lower classical energies than the ferromagnetic energy can be stable against small deformation, it is more difficult to decide which one of them is the ground state. In Sec. 6, we shall rely mainly on the calculation of classical energies $E'(\mathbf{Q})$ in predicting the order of these states. However, it is possible to obtain more definite conclusions in some respects. According to the discussion in Sec. 4, for instance, the exact energies of these antiferromagnetic states are in fact lower than the exact ferromagnetic energy at $T=0$, and, hence, the ferromagnetic state cannot be the ground state in these regions. The theorem in Sec. 4 also indicates that all states which have higher classical energies than the ferromagnetic energy are unstable. Consequently, we need to consider those metastable states whose classical energies are lower than the ferromagnetic energy.

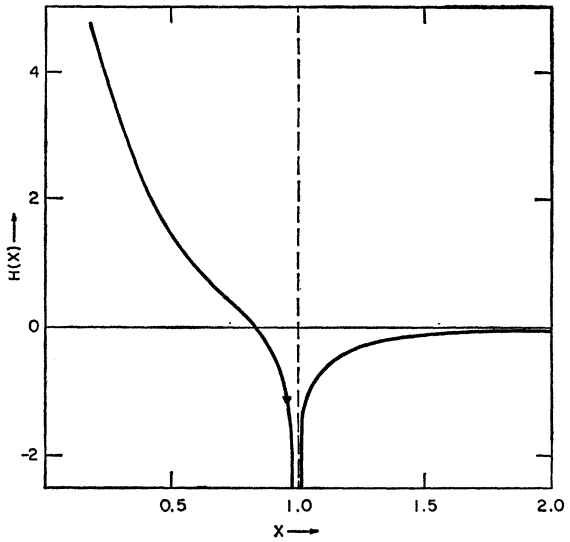

FIG. 2. Plot of $H(x)=U(x)/x+\partial U/\partial x$.

As it is not feasible to look for all possible metastable states, we shall limit our discussion in this paper to the following three antiferromagnetic states:

$$\mathbf{Q}_1=\frac{\pi}{a}\begin{pmatrix}1\\0\\0\end{pmatrix},\quad \mathbf{Q}_2=\frac{\pi}{a}\begin{pmatrix}1\\1\\0\end{pmatrix},\quad \mathbf{Q}_3=\frac{\pi}{a}\begin{pmatrix}1\\1\\1\end{pmatrix}. \quad (5.1)$$

The ferromagnetic energy $E(0)$ as well as the classical energies $E'(\mathbf{Q})$ of these three states are always extrema, since

$$[\partial E'(\mathbf{Q})/\partial\mathbf{Q}]=-\tfrac{1}{2}N[\partial I(\mathbf{Q})/\partial\mathbf{Q}]=0, \quad \text{for } \mathbf{Q}=0,\ \mathbf{Q}_1,\ \mathbf{Q}_2 \text{ and } \mathbf{Q}_3. \quad (5.2)$$

There may be other spiral structures which are metastable. For example, spin-wave spectra evaluated numerically by Woll and Nettel[7] suggest such a possibility in the hexagonal closed pack lattice, but we shall not investigate it in this paper.

There is a very important point to be discussed before applying the Green function method to those antiferromagnetic states. It is well recognized that the method can be applied without difficulties to the

"ground" state $\mathbf{Q}_0$ which has the lowest classical energy $E'(\mathbf{Q}_0)$. However, we find difficulties in calculating metastable states whose classical energies $E'(\mathbf{Q})$ are higher than the "ground" state energy $E'(\mathbf{Q}_0)$ but lower than the ferromagnetic energy $E(0)$. Although excitation energies $\epsilon_\nu(\mathbf{Q})$ of such states are real in the limit of small ν, showing the stability against small deformation, at finite ν the $\epsilon_\nu(\mathbf{Q})$ may become imaginary, because $I(\mathbf{Q})-I(\nu)$ in the parentheses on the right of Eq. (3.9a) turns to negative when $\nu\approx\mathbf{Q}_0$. It is also impossible to eliminate cases that the $F_\nu(\mathbf{Q})$ become negative, because $I(\mathbf{Q})$ is no longer an absolute maximum. Those imaginary or negative values are unpleasant to handle. In fact, the value of the probability of finding spin waves given by

$$\langle S_{\nu+}{}^{(\mathbf{Q})}S_{\nu-}{}^{(\mathbf{Q})}\rangle+\langle S_{\nu-}{}^{(\mathbf{Q})}S_{\nu+}{}^{(\mathbf{Q})}\rangle$$
$$=[\sigma^2(\mathbf{Q})F_\nu(\mathbf{Q})/\epsilon_\nu(\mathbf{Q})]\coth\tfrac{1}{2}\{\beta\epsilon_\nu(\mathbf{Q})\} \quad (5.3)$$

may become negative if $F_\nu(\mathbf{Q})$ is negative, and it is undetermined at $T=0$ if $\epsilon_\nu(\mathbf{Q})$ is imaginary since the expression on the right of Eq. (5.3) is written as

$$\lim_{\beta\to\infty}(-1)[\sigma^2(\mathbf{Q})F_\nu(\mathbf{Q})/|\,\epsilon_\nu(\mathbf{Q})\,|]\cot\tfrac{1}{2}\{|\,\beta\epsilon_\nu(\mathbf{Q})\,|\}. \quad (5.4)$$

The above situations illustrate apparent contradictions involved in the treatment and suggest the breakdown of the Green function method, because the value on the left of Eq. (5.3) should be positive by definition.

This limitation of the method may be serious in some problems, since we have to always carry out the calculation based on the "ground" state $\mathbf{Q}_0$. For instance, the total energy $E(\mathbf{Q}_0)$ calculated by (3.12) and (3.13) may not be the lowest, even though the classical energy is the minimum. Furthermore, it is difficult to apply the method in predicting a possible phase transition to another state, say $\mathbf{Q}$, at finite temperature, for the exact free energy of the state $\mathbf{Q}$ has to be calculated starting from the energy of the ground state $\mathbf{Q}_0$. If the phase transition would exist, a kink should appear in the free-energy curve and the long-range ordering of spins will change to that of the excited state $\mathbf{Q}$ beyond this kink. It is obvious that such an exact calculation is not feasible. What we would like to do, in practice, is to calculate an approximate free-energy curve pertinent to the excited state $\mathbf{Q}$ starting from the metastable state $\mathbf{Q}$ and neglecting the absolute minimum in the energy curve at $\mathbf{Q}_0$. It is really a serious drawback of the Green function method that phase transitions between ordered phases cannot be calculated in a conventional manner.

We shall now turn to the calculation of the relative stability condition that excitation energies are real in the limit of small ν. Use of (3.9c) and the assumptions (1) and (2) of Sec. 4, we expand $\epsilon_\nu(\mathbf{Q}_i)$ as follows:

$$\epsilon_\nu(\mathbf{Q}_i)=2\sigma(\mathbf{Q}_i)\{C_i[I(\mathbf{Q}_i)-I(0)]\}^{1/2}(\nu/2k_F), \quad (5.5)$$

where

$$C_i=-(k_Fa)D\sum_{\kappa_i*}\tfrac{1}{6}[g(\kappa_i*)]\{\mathcal{J}_{sf}{}^2(\kappa_i*)G(\kappa_i*/2k_F)$$
$$+4\mathcal{J}_{sf}(\kappa_i*)[(2k_F)\mathcal{J}_{sf}{}'(\kappa_i*)]H(\kappa_i*/2k_F)$$
$$+2[\mathcal{J}_{sf}(\kappa_i*)\,((2k_F)^2\mathcal{J}_{sf}{}''(\kappa_i*)\,)+((2k_F)\mathcal{J}_{sf}{}'(\kappa_i*)\,)^2]$$
$$\times U(\kappa_i*/2k_F)\}>0. \quad (5.6)$$

We have introduced a new variable $\boldsymbol{\kappa}_i*\equiv\mathbf{Q}_i+\boldsymbol{\kappa}$, and the $\{\boldsymbol{\kappa}_i*\}$ are then the reciprocal lattice vectors which are newly created over $\{\boldsymbol{\kappa}\}$ owing to the lower symmetry of the appropriate antiferromagnetic states. According to the theorem in Sec. 4, $I(\mathbf{Q}_1)-I(0)$ must be greater than zero for the state $\mathbf{Q}_i$ to be stable, and, hence, the condition that excitation energies are real in the limit of small ν is written as $C_i>0$ as it appears in Eq. (5.6). This relative stability condition is similar to (4.20) and (4.24), and is satisfied only for certain values of k_Fa. We shall again investigate three cases.

Case 1. Kasuya's $\mathcal{J}_{sf}(q)$

For the Kasuya-type functional dependence[9] we see immediately that the $\mathbf{Q}_i$'s, as well as any $\mathbf{Q}\neq0$ state, are never stable since from (4.16) we have

$$I(0)-I(\mathbf{Q})>0, \qquad \mathbf{Q}\neq0, \quad (5.7)$$

and hence antiferromagnetism is impossible for all k_Fa at any temperature.

Case 2. $\mathcal{J}_{sf}(q)=\mathcal{J}_{sf}(0)=$ constant

In the Mattis limit,[3] $I(\mathbf{Q}_i)-I(0)$ is no longer always negative, since $I(\mathbf{Q}_i)$ oscillates in a similar manner as $I(0)$. The numerical results in Sec. 6 will show, however, that the oscillation of $I(\mathbf{Q}_i)$ is out of phase with $I(0)$, demonstrating alternative appearances of ferro- and antiferromagnetisms. The relative stability condition (5.6) for the excitation energies is simplified as

$$-\sum_{\kappa_i*}g(\kappa_i*)G(\kappa_i*/2k_F)>0. \quad (5.8)$$

As is shown in Fig. 1, the value of $G(\kappa_i*/2k_F)$ for $\kappa_i*<2k_F$ is positive, and hence, the above conditions cannot be satisfied unless

$$\kappa_i*_{\min}<2k_F. \quad (5.9)$$

Consequently, the antiferromagnetic states cannot appear unless the following conditions are satisfied:

$$k_Fa>\pi/2 \quad \text{for} \quad \mathbf{Q}_1,$$
$$k_Fa>\sqrt{2}\pi/2 \quad \text{for} \quad \mathbf{Q}_2,$$
$$k_Fa>\sqrt{3}\pi/2 \quad \text{for} \quad \mathbf{Q}_3, \quad (5.10)$$

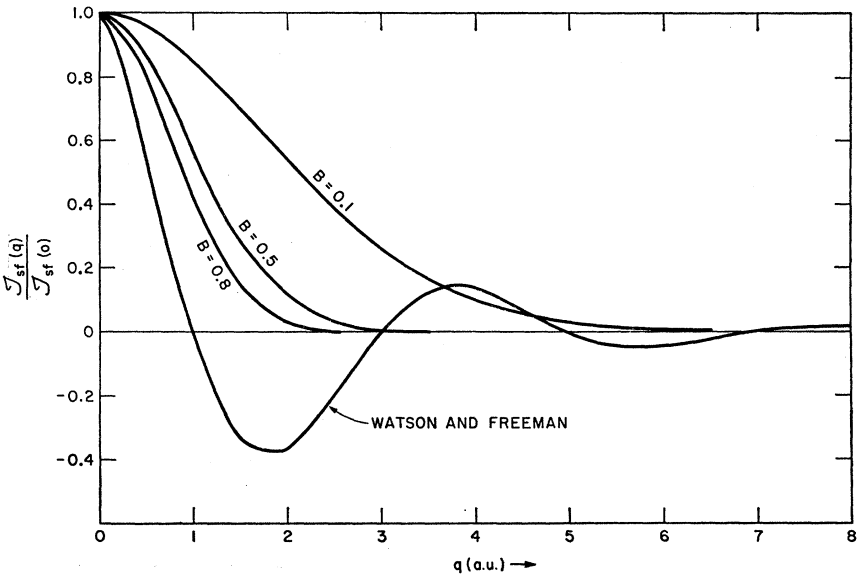

FIG. 3. Plot of various $\mathcal{J}_{sf}(q)/\mathcal{J}_{sf}(0)$ used in the calculation of $I(Q)$ versus q. The simply decaying curves are obtained from the expression $\mathcal{J}_{sf}(q)/\mathcal{J}_{sf}(0)=(1+q^2/16)^{-1}\exp(-Bq^2)$ with $B=0.1$, 0.5, and 0.8, while the curve obtained by Watson and Freeman is reproduced by the expression $\cos\frac{1}{2}(\pi q)\exp\frac{1}{2}(-q)$.

indicating the appearance of the ferromagnetic state for small values of k_Fa. For large k_Fa, however, C_i oscillates about zero in a similar manner as the expression on the left of Eq. (4.20), but effectively out of phase with it. The origin of this oscillatory behavior is again due to the Kohn anomalies in the spin-wave dispersion curve. More explicitly, the inequality (5.8) is violated for $k_Fa\gtrsim 2.5$ for Q_1, $k_Fa\gtrsim 3.2$ for Q_2, and $k_Fa\gtrsim 4.0$ for Q_3 because the second term on the left of Eq. (5.8) becomes dominant but still negative. Beyond the singularities of $G(\kappa_{i2}^*/2k_F)$, that is, $k_Fa\approx(\sqrt{5})\frac{1}{2}\pi$ for Q_1, $(\sqrt{6})\frac{1}{2}\pi$ for Q_2, and $(\sqrt{11})\frac{1}{2}\pi$ for Q_3, however, the second term turns positive, yielding the passing through of a kink in the limit $v\to 0$ of the dispersion curve. The inequality (5.8) is then satisfied again and so on.

Case 3. General $\mathcal{J}_{sf}(q)$

In the case of general $\mathcal{J}_{sf}(q)$, the relative stability condition (5.6) may be simplified to

$$-g(\kappa_{i1}^*)\mathcal{G}(\kappa_{i1}^*/2k_F)-\sum_{n=2}^{\infty}[\mathcal{J}_{sf}(\kappa_{in}^*)/\mathcal{J}_{sf}(\kappa_{i1}^*)]^2 \times g(\kappa_{in}^*)\mathcal{G}(\kappa_{in}^*/2k_F)>0. \quad (5.11)$$

As before, an antiferromagnetic state cannot occur unless the value of k_Fa exceeds the appropriate value listed in Eq. (5.10). As long as the value of $\mathcal{J}_{sf}(\kappa_{in}^*)$ decreases

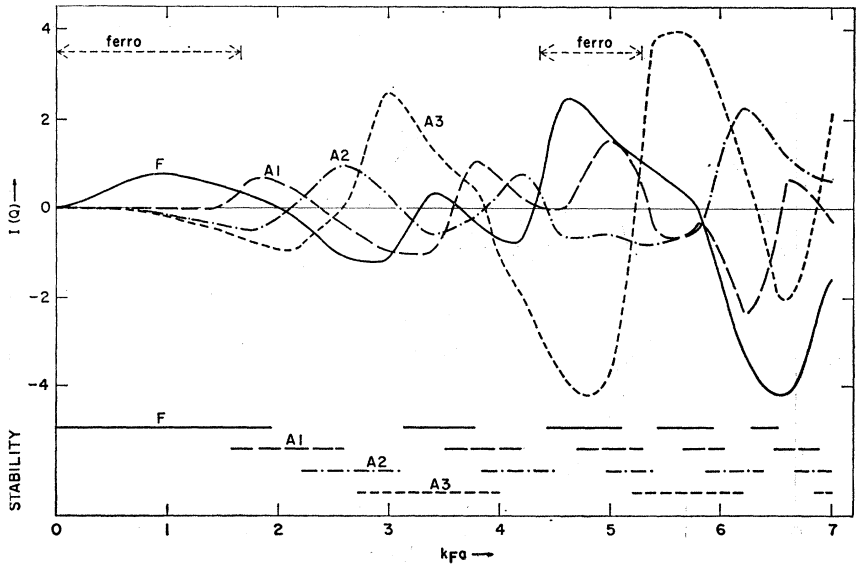

FIG. 4. Plot of $I(\mathbf{Q})$ versus k_Fa for the ferromagnetic state $\mathbf{Q}=0$ and the three antiferromagnetic states Q_1, Q_2, and Q_3. A constant $\mathcal{J}_{sf}(q)$ is assumed in the calculation. Regions of k_Fa where the relative stability condition is satisfied are illustrated in the lower part of the figure.

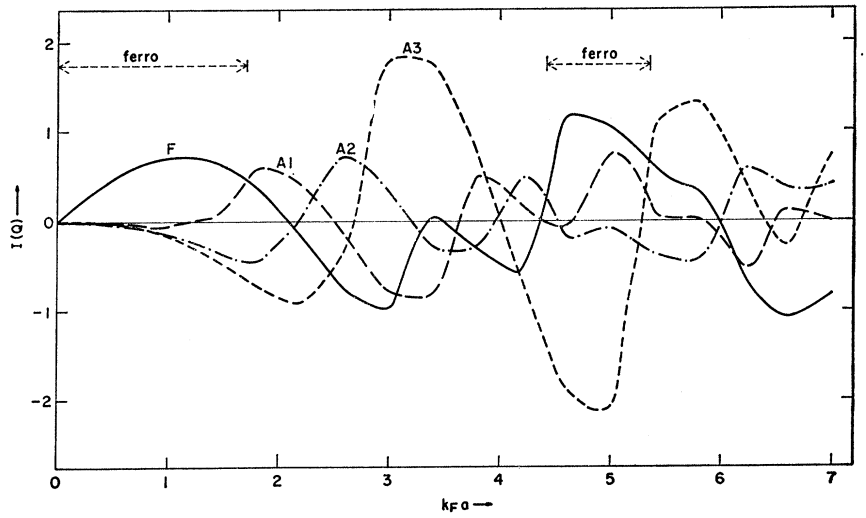

FIG. 5. Plot of $I(\mathbf{Q})$ versus $k_F a$ for the ferro- and antiferromagnetic states $\mathbf{Q}=0$, $\mathbf{Q}_1$, $\mathbf{Q}_2$, and $\mathbf{Q}_3$. The $B=0.1$ curve in Fig. 3 is assumed for $\mathcal{J}_{sf}(q)/\mathcal{J}_{sf}(0)$.

with increasing κ_{in}^*, $[\mathcal{J}_{sf}(\kappa_{in}^*)/\mathcal{J}_{sf}(\kappa_{i1}^*)]$ is less than 1, and it becomes increasingly difficult for the second term to dominate the first term on the left of (5.11). Therefore, the region where the antiferromagnetic state is stable becomes wider. Because of the drastic change in values at the singularities of $\mathcal{G}(\kappa_i^*/2k_F)$, however, the second term turns to positive, and the inequality (5.11) is satisfied at approximately the same point as the case where $\mathcal{J}_{sf}(q)$ is constant. Finally, the ith region of the antiferromagnetic state will continue up to the $(i+1)$th region, and the state becomes stable for all $k_F a$ beyond the ith region. This tendency is exactly parallel to that obtained for ferromagnetism.

6. RESULTS AND DISCUSSION

We turn in this section to a discussion of the magnetic ordering that results from the present model and, in particular, illustrate the drastic changes in ordering when various forms of $\mathcal{J}_{sf}(q)$ are introduced.

The numerical calculation has been carried out as follows: First we computed the values of $I(\mathbf{Q})$ for $\mathbf{Q}=0$, $\mathbf{Q}_1$, $\mathbf{Q}_2$, and $\mathbf{Q}_3$, and plotted the values versus $k_F a$ in Figs. 4 to 8. To compute the values, the expansion (4.15) is used and the following forms of $\mathcal{J}_{sf}(q)$ are assumed:

(1) $\mathcal{J}_{sf}(q)/\mathcal{J}_{sf}(0)=\text{const.}$

(2) $\mathcal{J}_{sf}(q)/\mathcal{J}_{sf}(0)=(1+q^2/16)^{-1}e^{-Bq^2}$;
$B=0.1$, 0.5, and 0.8.

(3) $\mathcal{J}_{sf}(q)/\mathcal{J}_{sf}(0)=\cos^2_{\frac{1}{2}}(\pi q)e^{-q/2}$. (6.1)

To illustrate the ranges of the interactions, the values of the above functions versus q are plotted in Fig. 3.

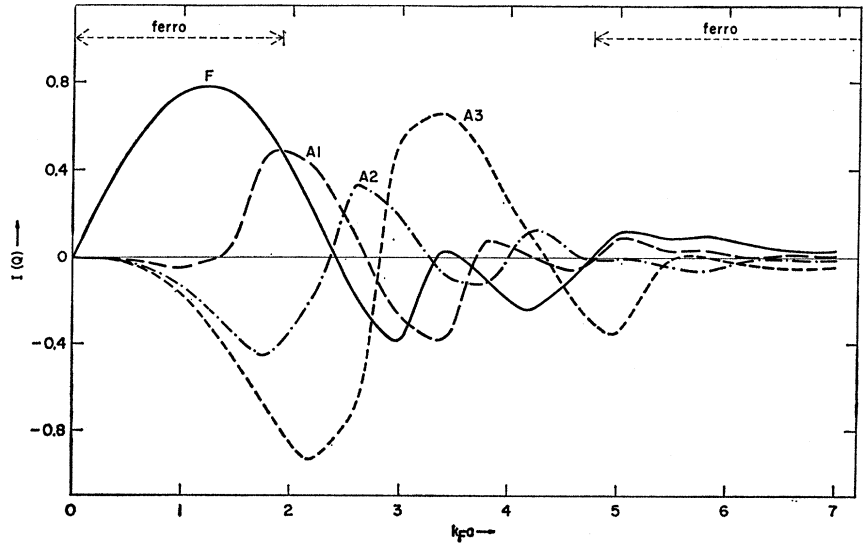

FIG. 6. Plot of $I(\mathbf{Q})$ versus $k_F a$ for the ferro- and antiferromagnetic states $\mathbf{Q}=0$, $\mathbf{Q}_1$, $\mathbf{Q}_2$, and $\mathbf{Q}_3$. The $B=0.5$ curve in Fig. 3 is assumed for $\mathcal{J}_{sf}(q)/\mathcal{J}_{sf}(0)$.

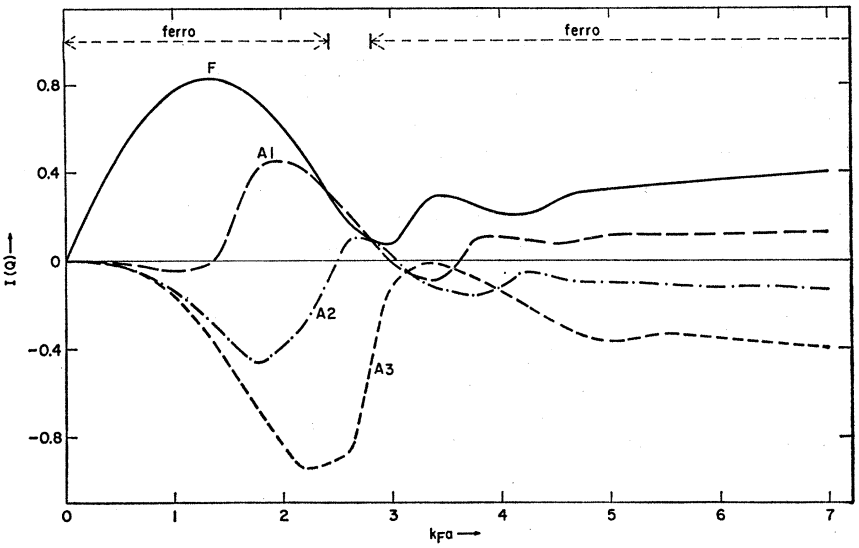

FIG. 7. Plot of $I(\mathbf{Q})$ versus $k_F a$ for the ferro- and antiferromagnetic states $\mathbf{Q}=0$, $\mathbf{Q}_1$, $\mathbf{Q}_2$, and $\mathbf{Q}_3$. The $B=0.8$ curve in Fig. 3 is assumed for $\mathcal{J}_{sf}(q)/\mathcal{J}_{sf}(0)$.

As is seen in the figure, case 3 fits to the numerical $\mathcal{J}_{sf}(q)$ obtained by Watson and Freeman[4] fairly well, while case 1 corresponds to the Mattis limit.[3] The three functions belonging to case 2 lie between those two extrema. In particular, we note that the one with $B=0.1$ resembles the J_{FF} obtained by Watson and Freeman by using the δ-function interaction and the Hartree-Fock atomic functions. The form of J_{FF} was originally suggested by Overhauser.[10]

As we have discussed in Eq. (5.2), the energies of the four states considered here are extrema. As long as no other states are stable, therefore we can read off the magnetic structure of the ground state with a particular $k_F a$ value in Figs. 4 to 8 by searching for the max $I(\mathbf{Q})$. In the regions of $k_F a$ where $I(0)$ is a maximum, the ferromagnetic state is all that can occur at any temperature since all antiferromagnetic states are unstable. The $I(0)$ in these regions also satisfies the condition (4.2), further confirming the stability of the ferromagnetism. In Figs. 4 to 8 these ferromagnetic regions are indicated by arrows connected by dotted lines and marked as "Ferro."

In the regions where $I(\mathbf{Q}_1)>I(0)$, one of the antiferromagnetic states may be the ground state. In the classical approximation, the state with maximum $I(\mathbf{Q})$ ought to be the ground state, but it is not certain if the ordering remains unchanged when the quantum correction $E''(\mathbf{Q})$ is included, and, hence, we shall not discuss it any longer. There are also some possibilities of observing transitions from the antiferromagnetic ground state to other excited states including the ferromagnetic excited state at finite temperatures.

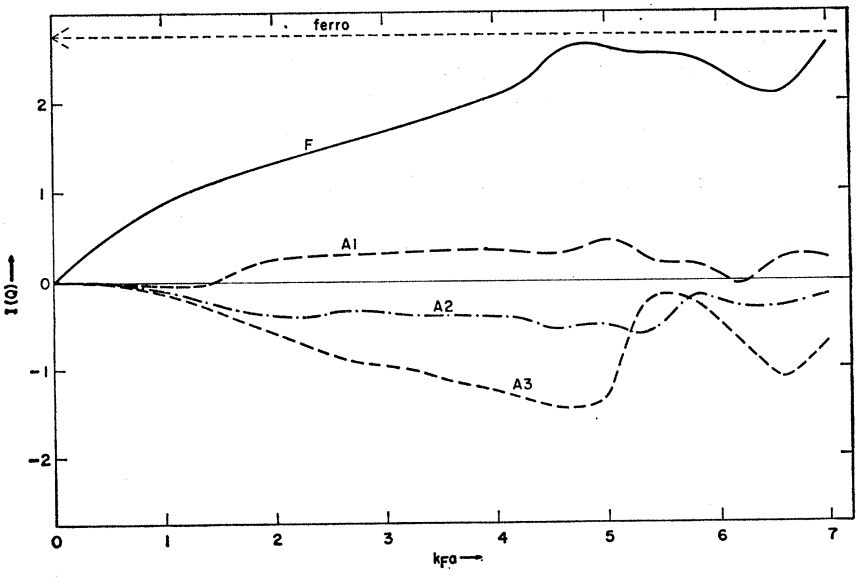

FIG. 8. Plot $I(\mathbf{Q})$ versus $k_F a$ for the ferro- and antiferromagnetic states $\mathbf{Q}=0$, $\mathbf{Q}_1$, $\mathbf{Q}_2$, and $\mathbf{Q}_3$. The Watson and Freeman curve in Fig. 3 is assumed for $\mathcal{J}_{sf}(q)/\mathcal{J}_{sf}(0)$.

Let us now examine the differences in the magnetic ordering patterns as a function of $\mathcal{J}_{sf}(q)$. Figure 4 shows the case where $\mathcal{J}_{sf}(q)$ is constant, while, in Fig. 5, the q dependence of the $\mathcal{J}_{sf}(q)$ resembles that of Overhauser. In those two cases, the patterns are essentially the same. In regions where $0<k_Fa\lesssim 1.7$, $4.4\lesssim k_Fa\lesssim 5.3$, etc., the ferromagnetic state appears. If the value of k_Fa increases gradually from 1.7 to 4.4, the antiferromagnetic states $A1$, $A2$, $A3$, $A1$, and $A2$ will appear one by one in the given order until, finally, the second ferromagnetic region follows. After the second ferromagnetic region, we observe again the antiferromagnetic states $A2$ and $A3$, and so on.

When the value of B involved in $\mathcal{J}_{sf}(q)$ increases, the range of the interaction $\mathcal{J}_{sf}(q)$ becomes narrower, and ferromagnetic regions tend to dominate over other states while the antiferromagnetic states gradually diminishes. This tendency is clearly shown in Figs. 6 and 7, and, finally, antiferromagnetic regions disappear completely for essentially all k_Fa in Fig. 8, where the $\mathcal{J}_{sf}(q)$ simulates the one given by Watson and Freeman. As is seen in Fig. 3, this $\mathcal{J}_{sf}(q)$ falls off very rapidly and is effectively equivalent to the $\mathcal{J}_{sf}(q)$ assumed by Kasuya.[9]

So far we have compared the total energies of the four distinct states $\mathbf{Q}$ to decide which one of them should appear as the ground state at a particular k_Fa value. Although those four states are energy extrema, we are not yet certain if they are energy minima or maxima in the vicinity of the pitch parameters $\mathbf{Q}$. To check the relative stability, we have calculated, in the case of constant $\mathcal{J}_{sf}(q)$, the expression on the left of the inequality (4.20) or (5.8), and illustrated the regions where this condition is satisfied in Fig. 4. As is seen from the results, the relative stability condition gives essentially the same results as the energy calculation, suggesting that the relative stability condition alone might give fairly complete information as to which of these four states becomes the ground state.

If this is the case, we might argue that the magnetic structure of the present system is intimately related to the Fermi surface through a mechanism which resembles the Kohn anomalies in spin-wave spectra. The reasons are as follows: When the values of k_Fa is small, ferromagnetism is stable and all antiferromagnetic states become unstable. As the value of k_Fa increases, however, the antiferromagnetic states $A1$, $A2$, and $A3$ appear one by one in the given order. The k_Fa values where the energy curves cross over and the change in the magnetic structure which takes place in Fig. 4 can be predicted by the simple relation $k_F=\kappa_i^*/2$ or $\kappa/2$ without the energy calculation. At $k_F=\frac{1}{2}\kappa_i^*$ or $\frac{1}{2}\kappa$, the expression on the left of Eq. (5.8) or Eq. (4.20) diverges, and, in the k_Fa region just beyond the divergence, the magnetic structure of the system changes to that of the state $\mathbf{Q}_i$ to which the reciprocal lattice vector $\boldsymbol{\kappa}^*$ or $\boldsymbol{\kappa}$ belongs.

As the Fermi surface deforms from the free-electron sphere, the value of k_F will change, and, hence, the regions where the relative stability condition for a particular state is satisfied will change. Consequently, we may find changes in the magnetic structure of the system.

As seen in Fig. 4, this simple criterion does not work so well for large k_Fa values even though the relative stability condition still reproduces the general tendency of the magnetic structure found by the energy calculation. There are also some exceptions such as the region $3.1<k_Fa<3.8$, where the relative stability condition predicts erroneously ferromagnetism even though antiferromagnetism is preferred energetically.

If the $\mathcal{J}_{sf}(q)$ decays with increasing q, the antiferromagnetic regions obtained from the stability condition (5.11) becomes wider while the energy calculation tends to narrow and finally diminish the antiferromagnetic regions. With a decaying $J_{sf}(q)$, therefore, the relevance of the Fermi surface to the stability of antiferromagnetic states becomes obscure, and in the Kasuya limit, no relation will remain because antiferromagnetism no longer appears. On the other hand, both the relative stability condition and the energy criterion yield wider regions for the stability of the ferromagnetism suggesting a more intimate relation between the Fermi surface and the ferromagnetic stability.

ACKNOWLEDGMENTS

The authors wish to thank Dr. J. E. Robinson for many helpful discussions, and Dr. B. Goodman, Dr. C. Herring, and Dr. D. C. Mattis for reading the manuscript.